

# An Analytic Study on Laminar Film Condensation along the Interior Surface of a Cave-Shaped Cavity of a Flat Plate Heat Pipe

**Jin Sung Lee\*, Tae Gyu Kim, Tae Sang Park, Choong Sik Kim**

*Computational Science & Engineering (CSE) Center, Samsung Advanced Institute of Tech.,  
Kyunggi-do 440-600*

**Chan Hoon Park**

*Samsung Electronics Co.*

An analytic approach has been employed to study condensate film thickness distribution inside cave-shaped cavity of a flat plate heat pipe. The results indicate that the condensate film thickness largely depends on mass flow rate and local velocity of condensate. The increasing rate of condensate film for circular region reveals about 50% higher value than that of vertical region. The physical properties of working fluid affect significantly the condensate film thickness, such as the condensate film thickness for the case of FC-40 are 5 times larger than that of water. In comparison with condensation on a vertical wall, the average heat transfer coefficient in the cave-shaped cavity presented 10~15% lower values due to the fact that the average film thickness formed inside the cave-shaped cavity was larger than that of the vertical wall with an equivalent flow length. A correlation formula which is based on the condensate film analysis for the cave-shaped cavity to predict average heat transfer coefficient is presented. Also, the critical minimum fill charge ratio of working fluid based on condensate film analysis has been predicted, and the minimum fill charge ratios for FC-40 and water are about  $\Psi_{crit} = 3\sim 7\%$ .  $\Psi_{crit} = 0.5\sim 1.3\%$ , respectively, in the range of heat flux  $q'' = 5\sim 90\text{ kW/m}^2$

**Key Words :** Cave-Shaped Cavity, Condensate Film, Flat Plate Heat Pipe, Fill Charge Ratio

## Nomenclature

<p><math>A</math> : Length of condensate flow on vertical region</p> <p><math>a^*</math> : Parameter defined by Eq. (12)</p> <p><math>a^+</math> : Parameter defined by Eq. (20)</p> <p><math>C_1, C_2</math>: Integral constants</p> <p><math>C^*</math> : Parameter defined by Eq. (16)</p> <p><math>C^+</math> : Parameter defined by Eq. (24)</p> <p><math>G</math> : Ratio of vertical flow length to circular radius, <math>A/R</math></p> <p><math>g</math> : Gravitational force</p>	<p><math>H</math> : Height of liquid pool</p> <p><math>h_{fg}</math> : Latent heat</p> <p><math>\bar{h}_m</math> : Average heat transfer coefficient</p> <p><math>k</math> : Thermal conductivity</p> <p><math>L</math> : Flow length on vertical wall</p> <p><math>m</math> : Condensate mass flow rate</p> <p><math>Q</math> : Heat transfer rate</p> <p><math>q''</math> : Heat flux</p> <p><math>R</math> : Radius of circular surface</p> <p><math>T</math> : Temperature</p> <p><math>u</math> : Velocity</p> <p><math>V_{in}</math> : Internal volume of vapor core per unit length</p> <p><math>V_l</math> : Total volume of working fluid per unit length</p> <p><math>V_p</math> : Volume of liquid pool per unit length</p> <p><math>V_\delta</math> : Volume of condensate film per unit length</p>
--	---

\* Corresponding Author,

E-mail : ljs86@sait.samsung.co.kr

TEL : +82-31-280-8251 FAX : +82-31-280-9158;

Computational Science & Engineering (CSE) Center,  
Samsung Advanced Institute of Tech., P. O. Box 111,  
Suwon, 440-600, Korea. (Manuscript Received July 27,  
2001; Revised March 7, 2002)

- length
- $X$  : Total flow length, defined in Eq. (33)
- $x$  : Vertical distance from horizontal axis
- $y$  : Normal distance from solid surface wall

**Greek symbols**

- $\delta$  : Condensate film thickness
- $\delta^*$  : Dimensionless liquid film thickness, defined in Eq. (11)
- $\delta^+$  : Dimensionless liquid film thickness, defined in Eq. (19)
- $\delta_v$  : Thickness of condensate film in vertical region, defined in Eqs. (16) and (24)
- $\bar{\delta}$  : Dimensionless thickness of condensate film at angle  $\theta = \pi/2$
- $\theta$  : Angle measured from positive vertical axis
- $\mu$  : Dynamic viscosity
- $\rho$  : Density
- $\Phi$  : Angle measured from positive horizontal axis  $X$
- $\Psi$  : Fill charge ratio of working fluid, defined in Eq. (28)
- $\Psi_{crit}$  : Critical minimum fill charge ratio of working fluid

**Subscripts**

- $crit$  : Critical
- $l$  : Liquid phase
- $v$  : Vertical
- $p$  : Pool

**1. Introduction**

Heat pipes have been used in various applications such as thermal control, heat exchangers, and electronic cooling. Especially, flat plate heat pipes have been made recently due to their advantages over conventional heat pipes, such as geometry adaption, ability for localized heat dissipation and the production of an entirely flat isothermal surface. Flat plate heat pipe was first introduced by Ooijen and Hoogendoorn(1979), and since then lots of studies have been accomplished. In general, the flat plate heat pipe has a rectangular shape of vapor core, and a wick is installed to the evaporator region to distribute uniformly the liquid over the entire surface so that

dry out is prevented. Most of the research works on the flat plate heat pipes focused on the analysis of vapor and liquid flow in the rectangular vapor channel and capillary wick. Mou and Gamal (1997) carried out the theoretical and experimental investigation of the flat plate heat pipe with rectangular vapor channel and capillary wick for an electronic cooling. Kamel and Mauricio(1991) presented an analysis of condensate flow with sintered wick and Tan et al. (2000) had carried out analytic works on liquid flows in an isotropic wick structure of a flat plate heat pipe with multiple heat source. It was found that the an-isotropic wick property and the heater location affected significantly the overall pressure and velocity distributions of the working fluid inside the heat pipe. Detailed analytical models and simulations for a asymmetric disk-shape and flat plate heat pipe were presented by Vafai and Wang(1992), and the liquid flow in the porous wicks and the vapor flow in the vapor region were later established and modified by Vafai et al. (1995). Vafai et al. reported the analytical results for the asymmetric vapor velocity profile, the vapor and liquid pressure distributions, and the vapor temperature distribution in the heat pipe. The effects of variations in the thickness of the vapor channel and the wick as well as the heat pipe on the performance of both disk-shaped and rectangular flat-plate heat pipe were analyzed. Also, Wang and Vafai(2000) conducted an experimental investigation of the thermal performance of a flat plate heat pipe. They found that the porous wick of the evaporator section creates the main thermal resistance resulting in the largest temperature drop, which affects consequently the performance of the heat pipe.

The flat plate heat pipe can be used to attain uniform temperature fields for a process of the manufacture. In this case, heat source is generally located bottom of the plate and with the help of the heat pipe, upper plate maintaining uniform temperature field can be obtained. In order to use a flat plate heat pipe as a uniform temperature field, more effective internal shape for a heat pipe is required. Conventional rectangular shape of internal structure lead to a very high thermal

resistance due to the accumulated condensate film, which is formed the upper part, lead to an undesirable effect on the uniform temperature field.

In the present study, an analytic approach has been employed to study condensate film thickness distribution inside cave-shaped cavity of a flat plate heat pipe. The cave-shaped cavity is a very effective internal structure of a flat plate heat pipe to accelerate condensate flow. Until comparatively lately, many works have been done for a laminar film condensation inside/outside vertical/horizontal tubes after the fundamental Nusselt's analysis. Krupiczka (1985), Wang et al. (2000) and Mossad (1999) studied on laminar filmwise condensation concerning the effect of the surface tension and gravity. The analysis on free and forced convection of laminar film condensation from a elliptic tube were performed by Memory et al. (1997), and Yang and Hsu (1997) performed an analytic research for local condensate film thickness under simultaneous effects of interfacial vapor shear and pressure gradient by adapting a geometry parameter of eccentricity.

In the present analysis, a theoretical analysis is carried out to understand the distribution of the condensate film in the cave-shaped wall. Using this model, the variations of condensate film thickness along the inner surface wall under various heat flux and temperature difference between vapor and wall for water and FC-40 as a working fluid are investigated. A correlation formula to predict mean heat transfer based on the present condensate the film analysis for cave-shaped wall is presented. Also, the minimum fill charge ratio of working fluid has been proposed based on the present condensate film analysis under various operating conditions.

**2. Analysis of Condensate Film Flow**

To understand the distribution of condensate film, the Nusselt's analysis of filmwise condensation can be applied for an inside cave-shaped wall. The physical model and coordinate system employed in the present analysis are shown in Fig. 1. The uniform wall temperature is below

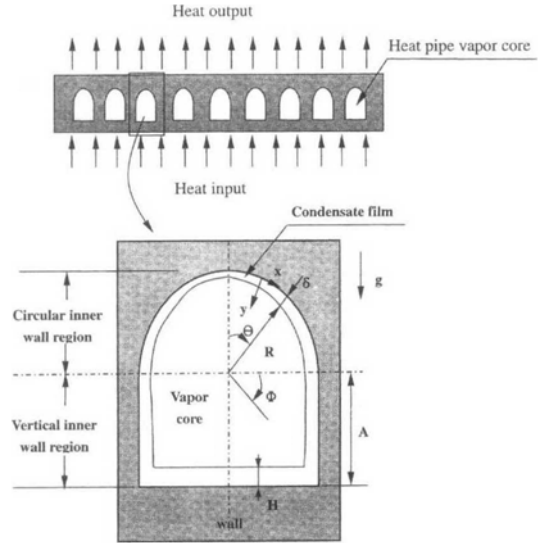


Fig. 1 Physical model and coordinate system

the saturation temperature. Thus, condensation occurs on the wall, and a continuous film of the liquid runs downward on the cave-shaped wall under the combined effects of gravity and shear force. Assumptions employed in the formulation of the problem are as follows: The condensate film is a laminar, steady flow and all physical properties of the condensate film are constant.

The velocity distribution  $u(y)$  at any location  $x$  across the condensate layer is determined by a force balance on a volume element as follows.

$$\mu \frac{d^2 u}{dy^2} + \rho g \sin \theta = 0 \tag{1}$$

Boundary conditions at the liquid-vapor interface and the wall are

$$\partial u / \partial y = 0 \text{ at } y = \delta, \quad u = 0 \text{ at } y = 0 \tag{2}$$

The integration of Eq. (1) subject to the boundary conditions gives the velocity distribution in the condensate layer:

$$u(y) = \frac{\rho g \sin \theta}{\mu} \left( \delta y - \frac{1}{2} y^2 \right) \tag{3}$$

The mass flow rate of condensate  $m(\theta)$  through any radial position  $\theta$  per unit width of the wall is given by

$$m(\theta) = \int_0^\delta \rho u dy \tag{4}$$

Introducing  $u$  from Eq. (3) into Eq. (4) and performing the integration yields

$$m(\theta) = \frac{\rho^2 g \delta^3 \sin \theta}{3\mu} \quad (5)$$

and differentiation with respect to  $\delta$  and  $\theta$  gives

$$dm = \frac{\rho^2 g \sin \theta}{\mu} \delta^2 d\delta + \frac{\rho^2 g}{3\mu} \delta^3 \cos \theta d\theta \quad (6)$$

The amount of heat released  $dQ$  over the area  $Rd\theta$  per unit length must be transferred across the condensate layer of thickness by conduction, therefore

$$dQ = h_{fg} dm = k \frac{\Delta T}{\delta} R d\theta \quad (7)$$

$$dm = \frac{kR\Delta T}{\delta h_{fg}} d\theta \quad (8)$$

Rearranging Eqs. (6) and (8), we obtain the following differential equation for the thickness of the condensate layer:

$$\left( \frac{\rho^2 g h_{fg}}{kR\mu\Delta T} \right) \delta^3 \sin \theta \frac{d\delta}{d\theta} + \frac{1}{3} \left( \frac{\rho^2 g h_{fg}}{kR\mu\Delta T} \right) \delta^4 \cos \theta = 1 \quad (9)$$

### 2.1 Constant wall temperature condition

*Circular inner wall region* ( $0 \leq \theta \leq \pi/2$ )

Introducing a dimensionless liquid film thickness  $\delta^*$  and a new parameter  $a^*$ , Eq. (9) can be rewritten in the following form:

$$\frac{3}{4} \sin \theta \frac{d\delta^*}{d\theta} + \delta^* \cos \theta = 1 \quad (10)$$

$$\text{where, } \delta^* = \frac{\delta^4}{a^*} \quad (11)$$

$$a^* = \frac{3Rk\mu\Delta T}{\rho^2 g h_{fg}} \quad (12)$$

Eq. (10) can be solved as follows:

$$\delta^*(\theta) = (\sin \theta)^{-3/4} \left\{ \frac{4}{3} \int (\sin \theta)^{1/3} d\theta + C_1 \right\} \quad (13)$$

*Vertical inner wall region* ( $\pi/2 < \theta$ )

The liquid film thickness on the vertical region can be calculated using the value at the angle of  $\theta=90^\circ$  as a boundary condition. Dimensionless liquid film thickness can be expressed as a function of the angle  $\Phi$  with respect to the horizontal axis.

$$\delta^*(\theta) = \frac{\delta_v^4}{a^*} + \bar{\delta} \quad (14)$$

$$= \frac{4}{3} \tan \Phi + \bar{\delta} \quad (15)$$

where  $\delta_v$  represents the liquid film thickness based on Nusselt's analysis on a vertical wall.

$$\delta_v^4 = C^* x \quad (16)$$

$$\text{where } C^* = \frac{4k\mu\Delta T}{\rho^2 g h_{fg}}, \quad x = R \tan \Phi, \quad \bar{\delta} = \delta^*_{(\theta=\pi/2)} \quad (17)$$

### 2.2 Constant heat flux condition

*Circular inner wall region* ( $0 \leq \theta \leq \pi/2$ )

Introducing a dimensionless liquid film thickness  $\delta^+$  and a new parameter  $a^+$ , Eq. (9) can be rewritten in the following form

$$\sin \theta \frac{d\delta^+}{d\theta} + \delta^+ \cos \theta = 1 \quad (18)$$

$$\text{where, } \delta^+ = \frac{\delta^3}{a^+} \quad (19)$$

$$a^+ = \frac{3q'' R \mu}{\rho^2 g h_{fg}} \quad (20)$$

Eq. (18) can be solved as follows:

$$\delta^+(\theta) = \frac{1}{\sin \theta} (\theta + C_2) \quad (21)$$

*Vertical inner wall region* ( $\pi/2 < \theta$ )

As mentioned earlier, the liquid film thickness on the vertical region can be calculated using the value at the angle of  $\theta=90^\circ$  as a boundary condition.

$$\delta^+(\theta) = \frac{\delta_v^3}{a^+} + \bar{\delta} \quad (22)$$

$$= \frac{4}{3} \tan \Phi + \bar{\delta} \quad (23)$$

where  $\delta_v$  represents the liquid film thickness based on Nusselt's analysis on a vertical wall.

$$\delta_v^3 = C^+ x \quad (24)$$

$$\text{where } C^+ = \frac{4q'' \mu}{\rho^2 g h_{fg}}, \quad x = R \tan \theta, \quad \bar{\delta} = \delta^+_{(\theta=\pi/2)} \quad (25)$$

### 3. Critical Minimum Fill Charge Ratio of Working Fluid

Because the working fluid fill charge ratio for a heat pipe affects predominantly on thermal performance, it is very important to determine the optimal fill charge ratio as a design parameter. For

a small quantity of fill charge ratio, it is easy to reach the dry-out limitation, but for an excess fill charge ratio, it results in an increasing of thermal resistance. In the present study, an investigation is conducted to calculate the critical minimum fill charge ratio of working fluid based on the analysis of condensate film flow. As shown in Fig. 1, the volume of the working fluid per unit length is the summation quantity of the working fluid as a liquid pool and a condensate film.;

$$V_t = V_p + V_s \tag{26}$$

$$V_t = \Psi V_{in} \tag{27}$$

where the fill charge ratio of working fluid  $\Psi$  is the ratio of the working fluid volume to the total internal volume.

$$\Psi = V_t / V_{in} \tag{28}$$

where  $V_{in} = \frac{\pi}{2} R^2 + 2AR$

Volume of the working fluid per unit length as a liquid pool and a condensate film are as follows:

$$V_p = 2HR \tag{29}$$

$$V_s = 2 \int_0^\theta \delta(\theta) dx \tag{30}$$

Thus, inserting Eqs. (27) ((30) into Eq. (26) yields

$$H = \Psi R \left( \frac{\pi}{4} + G \right) - \frac{1}{R} \int_0^\theta \delta(\theta) dx \tag{31}$$

where the value  $G$  means the ratio of the vertical flow length to the circular radius. The critical minimum fill charge ratio of working fluid can be predicted when the value of liquid pool get to  $H=0$  condition. Therefore,

$$\Psi_{crit} = \left\{ \frac{1}{R} \int_0^\theta \delta(\theta) dx \right\} / \left( \frac{\pi}{4} + G \right) \tag{32}$$

The Eq. (32) for critical minimum fill charge ratio of working fluid is derived by a simple mass balance between the liquid condensate quantity based on present analysis and the initial fill charge ratio. In the present analytic research, the evaporating heat transfer along the bottom surface have not been considered.

### 4. Results and Discussion

#### 4.1 Distribution of condensate film

Figures 2 and 3 show the values of dimensionless liquid film thickness versus the angle  $\theta$  for two conditions of constant wall temperature and constant heat flux. The integral constants for Eqs. (13), (21) can be found under the condition

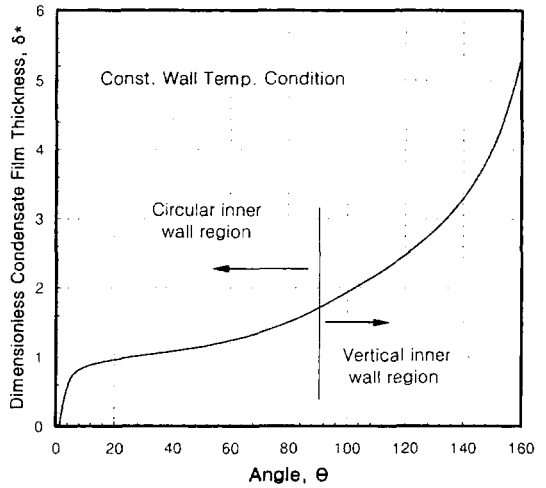


Fig. 2 Variation of dimensionless condensate film thickness as a function of the angle  $\theta$  for constant wall temperature condition

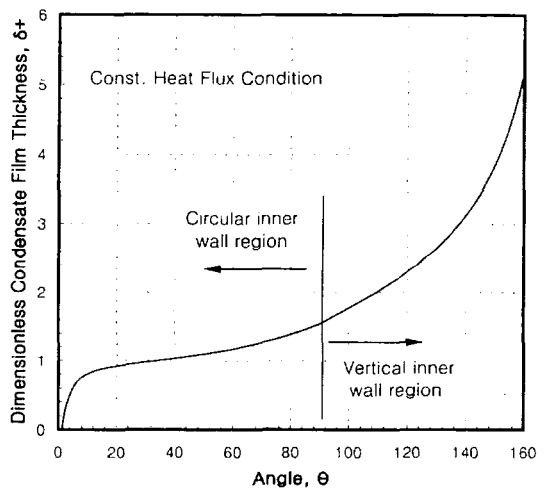


Fig. 3 Variation of dimensionless condensate film thickness as a function of the angle  $\theta$  for constant heat flux condition

of  $\delta^*(0) \cong 0, \delta^+(0) \cong 0$ . This boundary condition means that the condensate film originates at the top of the surface  $\theta=0$  and flows downward under the influence of gravity. Therefore the results presented in this study are valid only with this boundary condition. The variations of condensate film thickness near the top circular regions are increases dramatically, and as shown in Figs. 2 and 3, the condensate film thickness increases slightly beyond the angle of about  $\theta \cong 10^\circ$ . The thickness of the condensate film is determined by the balance of two effects: the condensation rate and the condensate film velocity. Hence, near the top of the circular region, the decreased effect of gravity (compared with the vertical wall) decreases the condensate velocity, resulting in a higher condensation rate, which tends to thicken the condensate film. The increased condensate film thickness results in a reduced condensation rate beyond that region and the increased effect of gravity, which tends to reduce the increasing rate of film thickness.

Figures 4 and 5 show the distribution of liquid film thickness using FC-40 as a working fluid. Figure 4 shows the variations of the condensate film thickness as a function of angle  $\theta$  under various temperature differences between vapor and wall. As shown in Fig. 4, the liquid film

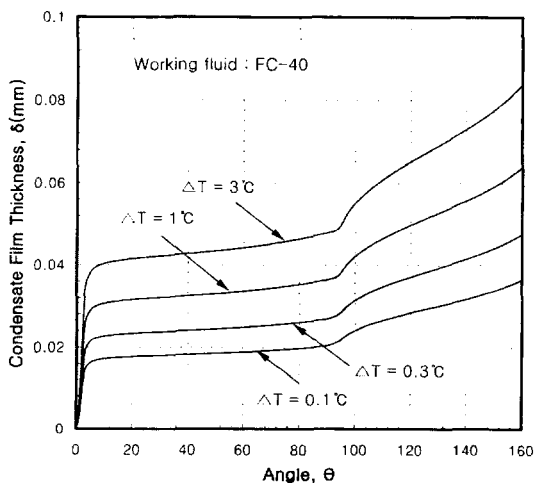


Fig. 4 Variations of condensate film thickness as a function of the angle ( under various temperature difference between vapor and wall

thickness varies in the range of 20~80μm. At the angle of  $\Phi=57.5$  with respect to positive horizontal axis, the flow length of the upper circular region and vertical region has a equivalent ones. The results show that the increasing rate of condensate for the circular region is about 50% higher value than that of the vertical region.

Figure 5 shows the variations of the condensate film thickness for the condensate film under various heat flux conditions. As the heat flux increases, high condensation rates appear having

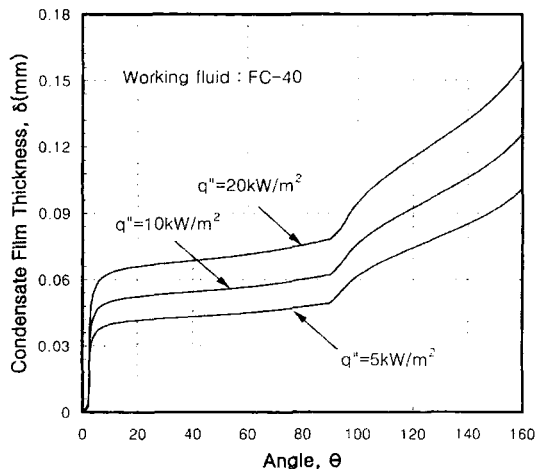


Fig. 5 Variations of condensate film thickness as a function of the angle  $\theta$  under various heat flux condition

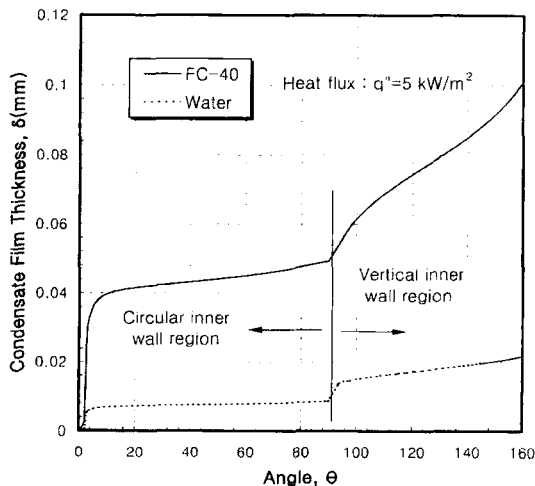


Fig. 6 Variations of the condensate film thickness for FC-40 and water as a working fluid

thicken the condensate film. Figure 6 shows the variations of the condensate film thickness for FC-40 and water as a working fluid. As shown in Fig. 6, there is a wide difference between two working fluids. FC-40, as a working fluid for a heat pipe, has a little advantage from a viewpoint of saturation pressure. For a comparatively high operating temperature above 100°C, its saturation pressure indicates lower value than other working

fluids. However, FC-40 is unsuitable as a working fluid for a heat pipe from a viewpoint of properties such as latent heat, thermal conductivity, viscosity etc. The value of the condensate film thickness for the case of FC-40 is 5 times larger than that of water.

From the distribution of the condensate film, it can be possible to predict the local heat transfer coefficient. Figure 7 shows the local heat transfer coefficients which were calculated based on the local condensate film thickness for various heat flux. Figure 8 presents the variations of the average heat transfer coefficient based on the Nusselt's analysis on a vertical wall and those of present study inside the cave-shaped wall from the local condensate film thickness. It indicates that the values of the average heat transfer coefficient in the cave-shaped wall are 10-15% lower value than those of the vertical wall. As mentioned earlier, the reason is that the average film thickness formed inside the cave-shaped wall was more thickened than that of the vertical wall with the equivalent flow length. The difference of average heat transfer coefficients between the vertical and the cave-shaped walls less as the value  $G$ , the ratio of circular radius and vertical length, increases. Eq. (33) is the correlation formula to predict the average heat transfer coefficient based on the present condensate film analysis for the cave-shaped wall.

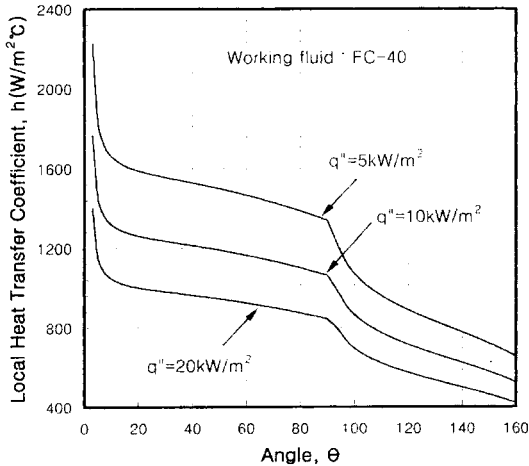


Fig. 7 Variations of local heat transfer coefficient as a function of the angle  $\theta$  under various heat flux condition

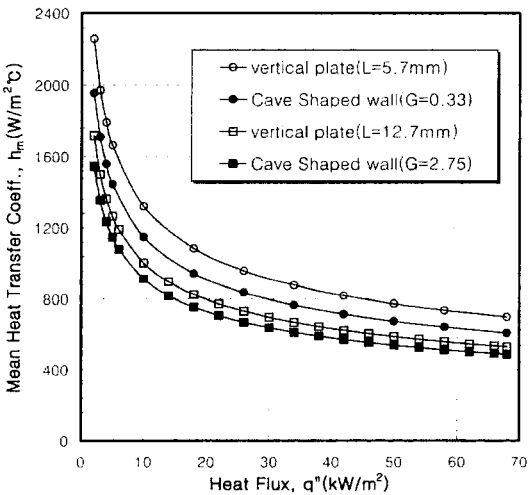


Fig. 8 Variations of mean heat transfer coefficient as a function of the heat flux for vertical wall and cave shaped wall with a equivalent flow length

$$\bar{h}_m = 0.798 \left( \frac{g \rho^2 h_{fg} k^3}{\mu q'' X} \right)^{1/3} \quad (33)$$

where  $X = R \left( \frac{\pi}{2} + \tan \phi \right)$

#### 4.2 Critical minimum fill charge ratio of working fluid

Fill charge of working fluid for a heat pipe affects on heat transport performance and heat transfer limitation. In case of a small quantity of working fluid, decreasing of thermal resistance results in enhancement of heat transfer performance, but it is easy to reach the heat transfer limitation due to the occurrence of dry-out in the evaporator region at the high heat flux. To prevent dry-out phenomenon, using of excess fill

charge of working fluid is more common, but this results in an increasing of thermal resistance and brings about unstable intermittent pulse boiling. A periodically rise of large mass of working fluid to the condenser region results in deterioration of thermal performance. Therefore, it is essential to determine an optimal fill charge ratio of working fluid considering the geometric shape and the operating condition of the heat pipe.

In the present study, a critical fill charge ratio

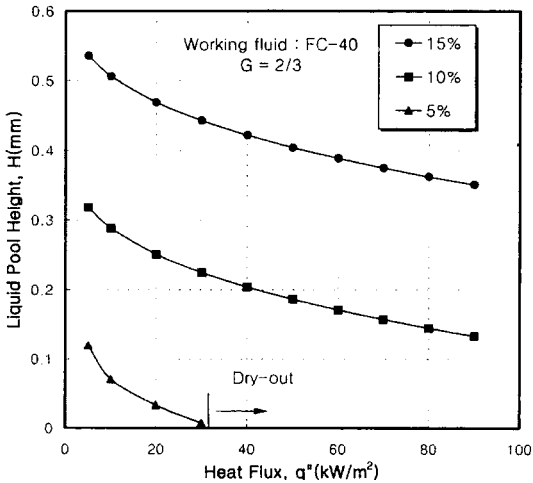


Fig. 9 Variations of liquid pool height in the evaporator region as a function of the heat flux

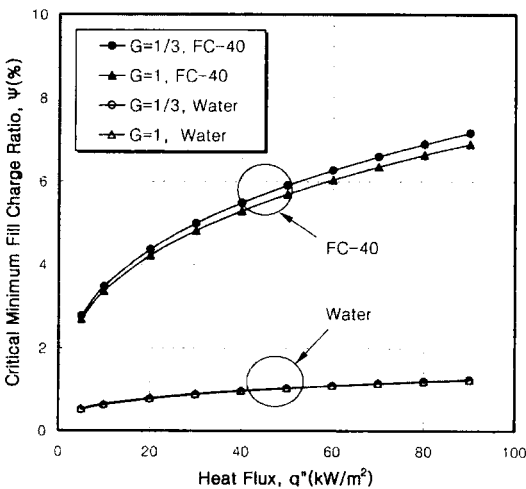


Fig. 10 Variations of the minimum fill charge ratio of working fluid as a function of the heat flux

of working fluid has been proposed based on the condensate film analysis inside the cave-shaped wall. Figure 9 shows the variations of liquid pool height in the evaporator region as a function of heat flux for various fill charge ratios of 5, 10 and 15%. The value of  $G$  means the ratio of vertical length to circular radius. As the heat flux increases, the height of liquid pool decreases gradually because of the increasing the condensate film thickness. The pool height gets to near "0" value at the heat flux of  $30 \text{ kW/m}^2$  for the fill charge ratio of 5%, so it can be possible to expect that it will bring about a heat transport limitation due to dry-out in the evaporator region. Figure 10 shows the variations of the fill charge ratio of working fluid as a function of the heat flux for various values of  $G$ . There is no significant difference appeared for various values of  $G$ . The minimum fill charge ratios for FC-40 and water are about  $\psi_{crit} = 3 \sim 7\%$ ,  $\psi_{crit} = 0.5 \sim 1.3\%$ , respectively, in the range of heat flux  $q'' = 5 \sim 90 \text{ kW/m}^2$ . As mentioned earlier, these values are obtained from the condition of the liquid pool height get reaching "0" value. Therefore, in the actual case, it is recommended practically to consider a little more excess of working fluid quantity than the present results.

### 5. Conclusions

In the present study, an analytic approach has been employed to study condensate film thickness distribution inside a cave-shaped cavity of flat plate heat pipe. Using the present model, a correlation formula for mean heat transfer coefficient is presented, and the critical minimum fill charge ratio of working fluid has been predicted under various operating conditions. Further experimental verification of these predicted trends for the cave-shaped cavity must be carried out by future researchers. From the present study, the following conclusions are obtained:

- (1) The condensate film thickness depends largely on the mass flow rate and local velocity of condensate. The increasing rate of condensate film for the circular region is about 50% larger value than that of the vertical region.



(2) The physical properties of working fluids affect significantly the condensate film thickness, such that the condensate film thickness for the case of FC-40 is 5 times larger than that of water.

(3) The average heat transfer coefficient in the cave-shaped wall is lower 10~15% than that of the vertical wall. A correlation formula of average heat transfer coefficient which is based on the present condensate film analysis for the cave shaped wall is as follows

$$\bar{h}_m = 0.798 \left( \frac{g \rho^2 h_{fg} k^3}{\mu q'' X} \right)^{1/3}$$

(4) The critical fill charge ratio of working fluid can be determined based on the condensate film analysis, and the minimum fill charge ratios for FC-40 and water are about  $\Psi_{crit} = 3 \sim 7\%$ ,  $\Psi_{crit} = 0.5 \sim 1.3\%$ , respectively, in the range of heat flux  $q'' = 5 \sim 90 \text{ kW/m}^2$

## References

- Kamel, A. R. and Mauricio, A. Z., 1991, "Modeling and Analysis of Flat Plate Heat Pipe with Sintered Wick," *Proceedings of the 7th Int. Heat Pipe Conference*, pp. 433~440.
- Krupiczka, R., 1985, "Effect of Surface Tension on Laminar Film Condensation on a Horizontal Cylinder," *Chem. Eng. Process*, Vol. 19, pp. 199~203.
- Memory, S. B., Adams, V. H. and Marto, P. J., 1997, "Free and Forced Convection Laminar Film Condensation on Horizontal Elliptical Tubes," *Int. J. of Heat and Mass Transfer*, Vol. 40, pp. 3395~3406.
- Mossad, M., 1999, "Combined Free and Forced Convection Laminar Film Condensation on an Inclined Circular tube with isothermal surface," *Int. J. of Heat and Mass Transfer*, Vol. 42, pp. 4017~4025.
- Mou, Q. and Gamal, M. G., 1997, "Theoretical and Experimental Investigation of Flat Plate Heat Pipe for Electronic Cooling," *Proceedings of the 10th Int. Heat Pipe Conference*.
- Ooijen, H. V. and Hoogendoorn, C. J., 1979, "Vapor Flow Calculations in a Flat Plate Heat Pipe," *AIAA Journal*, Vol. 17, pp. 1251~1259.
- Tan, B. K., Huang, X. Y., Wong, T. N. and Ooi, K. T., 2000, "A Study of Multiple Heat Sources on a Plate Heat Pipe Using a Point Source Approach," *Int. J. of Heat and Mass Transfer*, Vol. 43, pp. 3755~3764.
- Vafai, K. and Wang, W., 1992, "Analysis of Flow and Heat Transfer Characteristics of an Asymmetrical Flat Plate Heat Pipe," *Int. J. of Heat and Mass Transfer*, Vol. 35, pp. 2087~2099.
- Vafai, K., Zhu, N. and Wang, W., 1995, "Analysis of Asymmetric Disk Shaped and Flat Plate Heat Pipes," *J. of Heat Transfer*, Vol. 117, pp. 209~218.
- Wang, B. X. and Du, X. Z., 2000, "Study on Laminar Filmwise Condensation for Vapor Flow in an Inclined Small/Mini-Diameter Tube," *Int. J. of Heat and Mass Transfer*, Vol. 43, pp. 1859~1868.
- Wang, Y. and Vafai, K., 2000, "An Experimental Investigation of the Thermal Performance of an Asymmetrical Flat Plate Heat Pipe," *Int. J. of Heat and Mass Transfer*, Vol. 43, pp. 2657~2668.
- Yang, S. A. and Hsu, C. H., 1997, "Free and Forced Convection Film Condensation from a Horizontal Elliptic Tube with a Vertical Plate and Horizontal Tube as Special Cases," *Int. J. of Heat and Fluid Flow*, Vol. 18, pp. 567~574.